Applied Physics Express **9**, 026501 (2016)
http://doi.org/**10.7567/APEX.9.026501**

One-pass manufacturing of multimaterial colloidal particles using optical recognition-enhanced laser direct imaging lithography

Blaž Kavčič[1], Gašper Kokot[2], Igor Poberaj[3], Dušan Babić[3], and Natan Osterman[2*]

[1]*LPKF Laser & Electronics, d.o.o., 4202 Naklo, Slovenia*
[2]*Department of Complex Matter, J. Stefan Institute, 1000 Ljubljana, Slovenia*
[3]*Faculty of Mathematics and Physics, University of Ljubljana, 1000 Ljubljana, Slovenia*

*E-mail: natan.osterman@ijs.si

Received November 19, 2015; accepted December 8, 2015; published online January 5, 2016

We report on a maskless lithography rapid prototyping system for the fabrication of multimaterial hybrid structures in standard i-line negative photoresists enriched by the addition of functionalization particles. The system uses a combination of image recognition methods to detect particle positions in the photoresist and laser direct imaging to illuminate it with a focused ultraviolet laser. A set of acousto-optic deflectors, used to steer the laser, enables precise high-speed illumination of complex patterns. As a result, hybrid micron-sized structures composed of a base particle embedded in a photoresist frame can be manufactured using a one-pass process.

Many experiments involving colloids rely on particles with a specific shape and structure to exert different forces on the particles or to induce complex interactions between them. These non-spherical and non-isotropic particles can be used as model systems for a variety of fundamental phenomena in materials and soft matter;[1)] additionally, they enable a wide range of nano- and bio-photonic applications.[2)] Based on their type, they can be divided into three categories: shape-anisotropic particles with complex topology, internally structured particles made of multiple materials with different physical properties, and chemically-patterned particles carrying chemically distinct sites to aid chemical interactions.[3)] Specific particles can fall into two or three categories; for example, shape-anisotropic particles with embedded chemical reactants and magnetic nano-beads fall into three categories. This paper focuses on certain shape-anisotropic internally structured particles; however, in general, the presented manufacturing technique is applicable to fabrication of all three categories of complex particles.

A common technique for producing a large number of non-spherically symmetric colloidal particles is photolithography.[4,5)] This method uses a high-resolution patterned projection mask through which a thin layer of photoresist is exposed to a UV light source. Next, the photoresist is developed. Then, the produced particles are detached from the substrate and collected for further use. Multi-pass layer-by-layer processing enables the use of hybrid polymer particles with complex three-dimensional shapes and different internal compositions.[6)]

Mask-based photolithography has also been employed for direct synthesis of multifunctional microparticles with magnetic, amphiphilic, and anisotropic properties.[7)] Indirect synthesis of monodisperse, superparamagnetic, micron-sized prisms of arbitrary cross-section is possible by molding a dispersion of magnetic colloids in a UV-curable monomer in polydimethylsiloxane wells.[8,9)] For a review of recent experimental results related to the realization of anisotropic magnetic colloids, see.[10)]

Often, one needs heterostructures of arbitrary shape that include some pre-made particles that provide additional functionality. Examples of these functionalization particles are (para)magnetic beads for magnetic manipulation; fluorescent beads, which assist optical detection; and patchy particles with anisotropic interactions.[11)] Functionalization particles can be mixed into the photoresist and standard mask-defined photopolymerization can be used to pattern the heterostructures.[12)] However, these added particles are randomly scattered across the surface of the structure.

In this letter, we report on a system for one-pass sub-micrometer-resolution fabrication of heterostructured particles of arbitrary shape, size, and thickness. The heterostructured particles are functionalized at a desired position. In contrast to other fabrication methods, we first deposit the functionalization particles on a solid substrate before coating it with photoresist and performing the photolithography step. Because the positions of the functionalization particles are random, mask lithography cannot be used in this case. One fabrication method that avoids using masks is laser direct imaging (LDI) lithography.

LDI is a maskless lithography technique that uses a UV laser beam focused through a microscope objective with a high numerical aperture, and a precise beam steering mechanism to directly expose the photoresist surface to the desired pattern. Avoiding the use of masks speeds up the prototyping process and provides high flexibility in pattern alignment, orientation, and scaling (and therefore, matches its dimensions and position relative to the substrate). Having the ability to place the exposure pattern at any chosen position on the substrate surface is a crucial property of LDI and can be combined with an image recognition system to identify each randomly positioned functionalization particle on the substrate and expose it with a micro-particle pattern accordingly.

Our LDI setup uses a 375 nm UV laser (Omicron Laserage Bluephoton 375.20.CWA.L.WS, 375 nm, 16 mW) and a 20× objective (Zeiss LD Plan NEOFLUAR 20×/0.4 Korr), which results in a 1 μm spot size. A pair of acousto-optic deflectors (AODs) controls the beam intensity and position on the photoresist surface. Because AODs have no moving parts and are controlled by a digital frequency generator with precision better than 10^{-8}, the beam position and intensity can be changed in a random-access manner at up to 200 kHz with sub-nanometer beam positioning precision, which makes them faster and more precise than mechanical alternatives. The patterns are exposed as raster images in a point-by-point fashion, where the raster size (laser spot spacing) can be arbitrarily set so as to provide an optimal combination of exposure speed and pattern resolution. Additional details regarding the LDI setup can be found elsewhere.[13)]

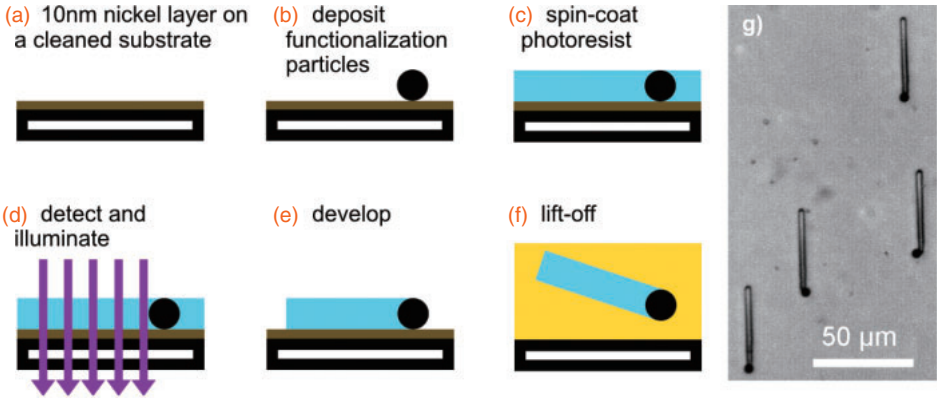

Fig. 1. (a–f) Schematic diagram of heterostructured particle fabrication process using laser direct imaging lithography. (g) Optical micrograph of several particles taken after the development step.

To prepare the substrate for particle fabrication, a 10-nm-thick nickel layer is first deposited on a clean microscope glass slide using a standard evaporation technique [Fig. 1(a)]. The nickel serves as a sacrificial layer to aid lift-off after the particles are fabricated. Its small thickness allows inspection of the sample surface using a transmission microscope. After nickel deposition, the substrate is treated in oxygen plasma for 10 s to increase its surface hydrophilicity. A drop of the functionalization microbeads suspension is then deposited on the substrate and smeared with a pipette tip. Once completely dry, the beads remain randomly scattered across the substrate surface at a surface density that is controlled via the density of the initial suspension [Fig. 1(b)]. The surface density of the beads is chosen to be large enough to produce a reasonable yield of particles while avoiding too many occurrences of neighboring particles in contact, or embedding more than one bead into a single heterostructured particle. A layer of negative photoresist is spin-coated onto the substrate over the beads using spin and bake parameters specified by the photoresist manufacturer to achieve the desired layer thickness [Fig. 1(c)].

The exposure of the photoresist follows. Our LDI setup is enhanced with an image recognition system that enables automated targeted exposure of pre-defined structures identified on the substrate. An image of a part of the substrate covered with functionalization beads and coated with a photoresist layer is first obtained. The area covered by the image corresponds to the working field size of the AODs, which is approximately $150 \times 150\,\mu m^2$. The image is analyzed to obtain the positions and sizes of all visible beads using standard video particle tracking methods for detection.[14] Particle agglomerations, dust particles, and other impurities are filtered out using a particle size criterion. Once the size and brightness parameters for the chosen photoresist and functionalization beads are manually tuned in the image recognition software, the detection and exposure processes run automatically and allow fabrication of a number of particles. The working field is exposed with a pre-defined particle-shape pattern at each position where a bead has been detected [Fig. 1(d)]. After the exposure, the translation stage moves by 150 µm and repeats the detection and exposure process. The process is repeated until an area of the required size has been covered.

After exposure, the photoresist is treated and developed following the procedure prescribed by the manufacturer, which reveals the structured photoresist particles with embedded functionalization microbeads [Fig. 1(e)]. The developed substrate is first treated in post-glow oxygen plasma to remove possible traces of undeveloped photoresist from the surface, and is then hard-baked. Figure 1(g) shows the typical situation after the hard-baking step. To detach the particles from the substrate an etchant is used [Fig. 1(f)]. A droplet of the etchant is carefully deposited on the spot with the fabricated particles. After the sacrificial layer is etched away, the free-floating particles are extracted with a pipette and undergo a four-cycle washing process, using a standard centrifuging technique to replace the etchant in the suspension with deionized water, and in turn, rendering the functionalized particle suspension ready for use.

The LDI lithography technique is used with an image recognition system, which makes it possible to use photolithography to fabricate functionalized micro-particles in an efficient way, despite random scatter of the functionalization beads across the substrate surface. For a typical fabrication process of particles with an approximate area of $100\,\mu m^2$, we set the LDI exposure grid raster size to roughly 0.25 µm. This setting provides a sufficiently high resolution for the chosen pattern and ensures that it has smooth sidewalls with a peak-to-peak roughness of the order of tens of nanometers, as predicted and confirmed experimentally by Koechlin et al.[15] At an AOD update frequency of 100 kHz, it takes roughly 20 ms to expose one particle. At the optimal functionalization bead surface density, the exposure takes less than 0.1 s per working field; the process is limited in speed primarily by the translation stage, whose positioning takes roughly 3 s per field. Including the initialization of the system, the exposure of a 10×10 array of working fields spanning $2.25\,mm^2$ and producing roughly 400 particles takes roughly 6 min to complete.

The use of the fabrication method described above can be demonstrated best using a recently performed experiment.[16] In our previous work, we showed that an externally driven artificial cilia array can be successfully used to pump a fluid flow.[17,18] A new experiment was designed to examine the hydrodynamic response of a passive biomimetic artificial cilium that is driven by an active artificial cilium. To further study the hydrodynamic coupling between such neighboring cilia, the behavior of a non-driven passive cilium, fabricated as a $40 \times 3 \times 3\,\mu m^3$ photoresist rod with an embedded

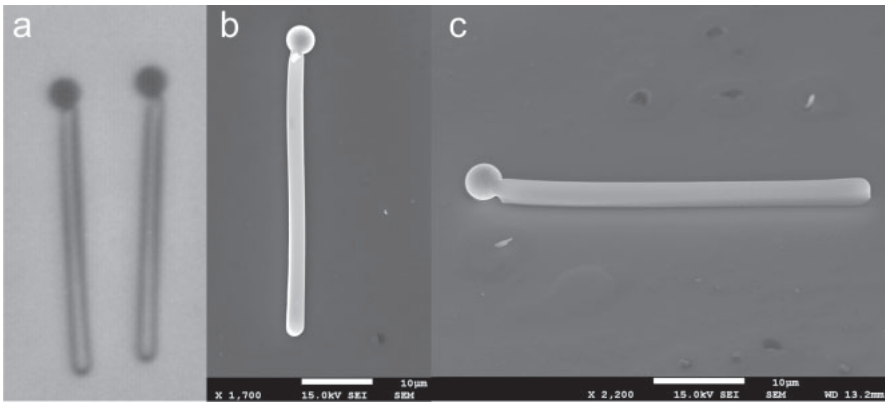

Fig. 2. Heterostructures made of $40 \times 3 \times 3\,\mu m^3$ photoresist rod and a 4.4 μm superparamagnetic bead. (a) Optical micrograph image; the beads are clearly distinguishable from the photoresist rods. (b) Top- and (c) side-view SEM images. Scale-bar is 10 μm.

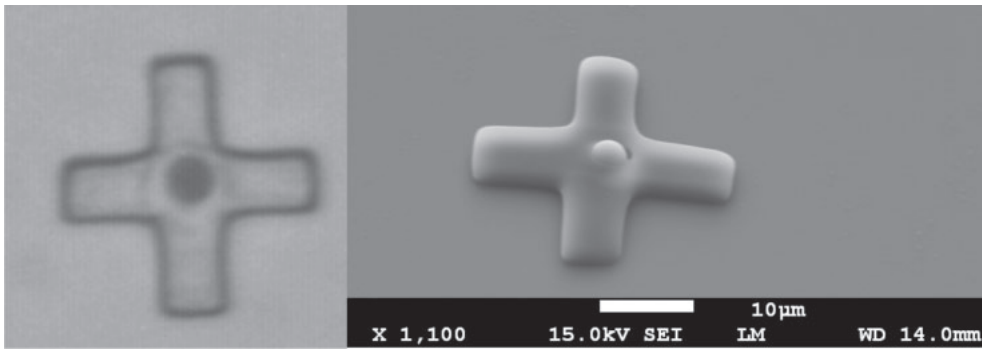

Fig. 3. Optical micrograph and SEM image of a heterostructure made of a superparamagnetic bead and a cross-shaped photoresist part. Scale-bar is 10 μm.

superparamagnetic bead at one end, was analyzed. Rod-like heterostructured particles can be anchored to pre-fabricated nickel anchoring sites by their magnetic ends, while remaining passive in an external magnetic field, unlike the driven cilia made of superparamagnetic bead chains.

For the functionalized particles, we used superparamagnetic microbeads with diameter 4.4 μm (Dynal Biotech Dynabeads M-450),[19] which were deposited on the nickel sacrificial layer substrate at a surface density of the order of 10^4 beads/cm^2, or approximately 4 beads per AOD working field. The deposited beads and the substrate were coated with a 3-μm-thick layer of negative photoresist (Microchemicals SU-8 2025), which was then soft-baked on a hot plate at 95 °C for 2 min.

The pattern used for LDI exposure was a rod-like rectangle $40 \times 3\,\mu m^2$ in size. Using the exposure parameters presented above, it took roughly 6 min to expose 400 particles. After exposure, the substrate was post-baked for 75 s at 95 °C and developed using a commercially available developer (Microchemicals mr-Dev 600). The substrate was treated in post-glow oxygen plasma for 80 s and then hard-baked for 60 min at 200 °C. Ultimately, the particle suspension was extracted using an etchant to remove the sacrificial nickel layer and washed. The fabrication process took roughly 2 h in total, including the hard-bake time, and ultimately yielded roughly 100 usable particles.

Figure 2 shows an optical micrograph and scanning electron microscopy (SEM) images of the produced multi-material particles. The heterostructure of each particle is clearly visible: a darker superparamagnetic polystyrene bead is embedded in a rod of cured photoresist. The high-contrast SEM image shows that the photoresist rod is attached to the bead at one end. Thus far, experiments using the produced particles show that the bond between the two is strong and is not easily broken. The same image also reveals that one side of the rod is not completely straight. The observed bending is the result of the rinsing step of the photoresist development process. Another example of microparticles of a different size, shape, and functionalization are shown in Fig. 3.

The yield of the fabrication process we currently use is only roughly 20%. This fraction of identified and exposed functionalization microbeads is successfully produced and can be extracted in the form of ready-for-use functionalized particles. There are several reasons for the low yield. Initial deposition of functionalization beads results in several multi-bead aggregates that can be mistakenly identified as a single particle, and consequently, exposed. A solution would be to use a more controlled method of deposition, e.g., employing self-assembly at liquid–liquid interfaces[20,21] to produce non-close-packed patterns of functionalization particles.

Functionalization beads that appear at the edge of the illuminated field may appear again at the opposite edge because of imperfect translation stage positioning, thus leading to a double exposure. In some cases, contamination of the surface with dust can also lead to undesired exposure events. An unwanted overlap of two exposed regions can also occur as a result of either an exceedingly high bead surface density or close spacing because of the random nature of the deposition process. The photoresist development step is

critical because, for some beads, the photoresist particles or whole heterostructures can be washed away by the developer. Among the remaining structures, some are distorted by strong fluid flows during the development process.

Despite the low yield of the production process, the number of fabricated heterostructured particles meets the functional requirements. For higher yields and higher production rates, the process can be significantly improved by setting stricter conditions for detection and exposure of the particles. Additionally, more advanced detection and exposure algorithms can be used. The photoresist substrate adhesion and the development procedure can also be optimized. Moreover, the process can be modified or upgraded to produce particles with functionalization of different chemical composition, shape, and size. The particles can be of a non-symmetric shape and can be produced using a photoresist that is also functionalized. To produce quasi three-dimensional particles, the photoresist coating, exposure, and development steps can be performed several times in succession prior to particle lift-off.

Optical recognition-enhanced laser direct imaging has proven to be a flexible tool for lithographic fabrication of complex structures because of its high speed and the customizability of the exposure pattern and parameters. Avoiding projection masks enables much simpler and faster alignment of the pattern with the substrate. The process is performed automatically by software, rather than mechanically, which is the key to achieving both high fabrication rates and the ability to work with a substrate that has a random (rather than a periodic) structure.

Micro-particles produced this way can be made of different photoresist materials; can be of arbitrary shape, size, and thickness; and can be functionalized with a variety of materials, for example fluorescent microbeads or superparamagnetic spheres. Once the size and brightness parameters of the chosen photoresist and functionalization beads have been manually tuned in the image recognition software, the detection and exposure processes run automatically and allow fabrication of a number of multimaterial hybrid particles.

Acknowledgments We thank P. Panjan for the Ni-coated substrates and acknowledge financial support from the Slovenian Research Agency (Grant Nos. J1-6724 and P1-0192). This work was supported in part by the European Social Fund of the European Union.

1) A. van Blaaderen, Nature **439**, 545 (2006).
2) J. Du and R. K. O'Reilly, Chem. Soc. Rev. **40**, 2402 (2011).
3) S.-M. Yang, S.-H. Kim, J.-M. Lim, and G.-R. Yi, J. Mater. Chem. **18**, 2177 (2008).
4) D. Brambley, B. Martin, and P. D. Prewett, Adv. Mater. Opt. Electron. **4**, 55 (1994).
5) D. Dendukuri, D. C. Pregibon, J. Collins, T. A. Hatton, and P. S. Doyle, Nat. Mater. **5**, 365 (2006).
6) C. J. Hernandez and T. G. Mason, J. Phys. Chem. C **111**, 4477 (2007).
7) S. Q. Choi, S. G. Jang, A. J. Pascall, M. D. Dimitriou, T. Kang, C. J. Hawker, and T. M. Squires, Adv. Mater. **23**, 2348 (2011).
8) J. W. Tavacoli, P. Bauër, M. Fermigier, D. Bartolo, J. Heuvingh, and O. du Roure, Soft Matter **9**, 9103 (2013).
9) I. Kavre, G. Kostevc, S. Kralj, A. Vilfan, and D. Babič, RSC Adv. **4**, 38316 (2014).
10) P. Tierno, Phys. Chem. Chem. Phys. **16**, 23515 (2014).
11) E. Bianchi, R. Blaak, and C. N. Likos, Phys. Chem. Chem. Phys. **13**, 6397 (2011).
12) D. C. Pregibon, M. Toner, and P. S. Doyle, Langmuir **22**, 5122 (2006).
13) B. Kavčič, D. Babić, N. Osterman, B. Podobnik, and I. Poberaj, Microsyst. Technol. **18**, 191 (2012).
14) J. C. Crocker and D. G. Grier, J. Colloid Interface Sci. **179**, 298 (1996).
15) M. Koechlin, G. Poberaj, and P. Günter, Rev. Sci. Instrum. **80**, 085105 (2009).
16) G. Kokot, M. Vilfan, A. Vilfan, I. Poberaj, and D. Babič, in preparation.
17) M. Vilfan, A. Potocnik, B. Kavcic, N. Osterman, I. Poberaj, A. Vilfan, and D. Babic, Proc. Natl. Acad. Sci. U.S.A. **107**, 1844 (2010).
18) M. Vilfan, G. Kokot, A. Vilfan, N. Osterman, B. Kavčič, I. Poberaj, and D. Babič, Beilstein J. Nanotechnol. **3**, 163 (2012).
19) G. Fonnum, C. Johansson, A. Molteberg, S. Mørup, and E. Aksnes, J. Magn. Magn. Mater. **293**, 41 (2005).
20) L. Isa, K. Kumar, M. Müller, J. Grolig, M. Textor, and E. Reimhult, ACS Nano **4**, 5665 (2010).
21) N. Vogel, C. K. Weiss, and K. Landfester, Soft Matter **8**, 4044 (2012).